Digest Journal of Nanomaterials and Biostructures Vol. 16, No. 4, October-December 2021, p.1329-1340

Preparation of La-Nd co-doped ZnO nanospheres and application on effluent treatment containing reactive dyes

L. Q. Cao, L. M. Wang*, M. R. Xie, L. H. Xu*, Y. Shen, H. M. Hao
School of Textiles and Fashion, Shanghai University of Engineering Science, Shanghai 201620, China

Zinc oxide (ZnO) nanospheres and La-Nd co-doped spherical ZnO composite were prepared by solvothermal method with zinc chloride and urea, ethylene glycol (EG) as morphology controller, to obtain excellent photocatalytic effect and degradation of pollutants containing reactive dyes. The morphology, structure and chemical composition were described by scanning electron microscopy (SEM), X-ray diffractometry (XRD), X-ray photoelectron spectroscopy (XPS) and diffuse reflection spectrum (DRS). The results showed that the size of La-Nd co-doped spherical ZnO about 130 nm, and the XRD results showed sharper characteristic peak. Meanwhile, the band gap of 2%La-1%Nd co-doped ZnO reduced from 3.23 eV to 2.97 eV. The degradation of effluent treatment containing reactive dyes like reactive red 24 (RR24) or reactive yellow 145 (RY145) was reached 99.99% under UV illumination for 75 min with 2%La-1%Nd co-doped ZnO as catalyst, which showed remarkable photocatalytic performance. After 120 min, removal efficiencies of chemical oxygen demand (COD) and total organic carbon (TOC) for RR24 discharge liquid attained 76.68% and 73.16% respectively, meanwhile, COD and TOC removal efficiencies for RY145 discharge liquid reached 76.32% and 72.36%.

(Received July 30, 2021, Accepted October 20, 2021)

Keywords: ZnO nanosphere, La-Nd co-doped, Photocatalysis, Reactive dye, Effluent treatment

1. Introduction

In recently years, pollutants in textile wastewater have attained great concern within scientific due to the trouble of degradation [1]. Reactive dyes possess high reactivity with cellulose and protein, which are widely used by the textile industry [2]. However, about 30% of the reactive dyes are wasted and contributing to the dyeing effluent because of dyes producing the hydrolysed reactive dyes [3]. Reactive red 24 (RR24) and reactive yellow 145 (RY145) are one of the most common reactive dyes in textile production. As reactive dyes, molecule of reactive red 24 only serves a monochlorotriazine as active group, however, reactive yellow 145 molecule provides a monochlorotriazine and a vinylsulfone. By comparison, the bifunctional structure of RY145 represent more complications, on the one hand, this characteristic makes the dyes easier to be adsorbed by catalysts, which increases the degradation rate to a certain extent, on the other hand, RY145 would be degraded with difficulty because of its intricate molecular structure.

Nano zinc oxide (ZnO) is considered to be a photoelectric semiconductor with high exciton binding energy, which possesses substantial thermal and chemical stabilities. Energy gap (Eg) of this material is found to be 3.37eV at room temperature [4], and when Irradiation with light (hv) ≥ Eg, photocarriers are produced by transiting of the photogenerated electrons from valence band to conduction band [5]. The hydroxyl radicals created by redox reaction of the carriers with

* Corresponding author: nirvanaclq@163.com

materials on the surface of ZnO are highly oxidizing [6], which can mineralize almost all organics without selectivity. Therefore, nano zinc oxide act as an important material that degrade textile wastewater containing reactive dyes [7-9].

Along with dyes, pollutants in discard solutions also include sodium salts which promote dyeing and auxiliaries with various functions. In such context, the addition of surfactants will enhance the chemical oxygen demand (COD) of liquors significantly [10]. Meanwhile, the presence of sodium chloride, sodium sulphate and other inorganic salts will affect the solubility of the dye [11], which exerts negative effect on photocatalysis degradation. Hence, limited degradation capacity with single ZnO impels us probe news ways to improve degradation rate. Nithya [12] et al reported that Mn-doped ZnO NPS (Zinc Oxide nanoparticles) were successfully prepared and loaded on cotton stalk activated carbon by chemical precipitation method, which showed improved photocatalytic activity. Balakrishna [13] et al prepared Ni -doped ZnO nanoparticles by the facile electrochemical method and obtained a great photocatalyst under UV light radiation. Christy [14] et al reported the preparation of Zr doped ZnO via sol-gel technique and discuss the degradation efficiency with reactive red 141 and reactive yellow 105, the results showed that 4% Zr doped ZnO nanocomposites has remarkable and enhanced degradation efficiency. Alam[15]et al doped with La, Sm, Dy and Nd respectively, and researched the photocatalytic performance of ZnO doped with various element, the results proved that doping improved the photocatalytic effect. These studies, though, reported that doping with rare elements is an effective method to decrease the band gap and enhance photocatalysis, however, the effects of co-doped of multiple elements and different morphologies on the photocatalytic of ZnO were seldom researched [16-18].

In this paper, in order to investigate the effects of morphology and element co-doping of ZnO on photocatalytic efficiency and wastewater treatment containing reactive dyes, the degradation effects of different morphologies and different doping ratios of two elements were studied. Spherical nano-sized ZnO was successfully prepared by solvothermal method by controlling the molar ratio of zinc chloride and ethylene glycol, and the purpose of improving photocatalytic efficiency and degrading effluent treatment containing reactive dyes was obtained by doping La and Nd [19]. Meanwhile, the excellent photocatalytic performance of this materials was proved by the degradation of the dyes and organic adjuvants [14-16], and the effect of inorganic sodium salts degradation of reactive dyes was explained by comparing the difference of dyes concentration between pure dye solution and effluent liquors at the same illumination time [17-19].

2. Materials and Methods

2.2. Materials

Zinc chloride, urea, ethylene glycol, lanthanum nitrate hexahydrate, neodymium nitrate hexahydrate, sodium chloride, sodium sulphate and sodium carbonate were purchased from Sinopharm Chemical Reagent Co. Ltd and were used as received. The dyes used for photocatalysis text were reactive red 24 and reactive yellow 145 (Novacron). Besides, penetrating agent JFC and peregal O(Demchem) were employed for the simulation of discard solutions. Deionized water was used in all the experiments.

2.3. Methods

2.3.1. Preparation of nano ZnO

A certain amount of ethylene glycol (the molar ration of zinc chloride to ethylene glycol was 1:0, 1:50, 1:100, 1:150, 1:200) as morphology control agent was mixed with deionized water respectively, then 0.3003 g urea and 0.1363 g zinc chloride were added into 30 mL of the blended

solvent successively. After the system was dispersed by magnetic stirring for 15 min, the mixture was transferred to a reactor and heated at 85 ℃ for 24 h. At the end of the reaction, resultant was centrifuged and the retained precipitate was washed three times with deionized water and anhydrous ethanol respectively, stoved at 65 ℃ for 8 h, afterwards, fully ground to obtain the powdered sample.

2.3.2. Preparation of La-Nd/ZnO

Refer to the preparation of ZnO, finite amounts of lanthanum nitrate hexahydrate and neodymium nitrate hexahydrate were served as precursors of the elements to be doped, according to formula: (X1, X2) = (nLa/nZn, nNd/nZn), the specific dosage was shown in Table. 1. After 30 min of continuous stirring, the evenly dispersed system was heated in a reaction kettle, then La-Nd modified ZnO samples with different incorporating ratios could be gained through washing, drying and grinding sequentially of the precipitates obtained by centrifuging.

Table 1. La-Nd co-doping amount.

doping ratio	lanthanum nitrate hexahydrate (0.01 mol/L)	neodymium nitrate hexahydrate (0.01 mol/L)
3.0%La-0.0%Nd	0.030mmol (3.0mL)	/
2.5%La-0.5%Nd	0.025mmol (2.5mL)	0.005mmol (0.5mL)
2.0%La-1.0%Nd	0.020mmol (2.0mL)	0.010mmol (1.0mL)
1.5%La-1.5%Nd	0.015mmol (1.5mL)	0.015mmol (1.5mL)
1.0%La-2.0%Nd	0.010mmol (1.0mL)	0.020mmol (2.0mL)
0.5%La-2.5%Nd	0.005mmol (0.5mL)	0.025mmol (2.5mL)
0.0%La-3.0%Nd	/	0.030mmol (3.0mL)

2.3.3. Characterization

Surface morphologies of ZnO were examined by using Zeiss Merlin Compact field emission scanning electron microscope, meanwhile the distribution of particle sizes could be observed. The crystallinity of powdered samples was characterized by X-ray diffraction (XRD) technique with Panaco X'pert Powder X-ray diffractometer in the diffraction angle range 2θ = 20-70 ° using Cu Kα radiation. The chemical state of the La-Nd co-doped ZnO was tested by X-ray photoelectron spectroscopy (XPS,), Al Kα radiation as the source (12 kV, 6 mA, vacuum> 5.0E-7mBar), Optical properties of La-Nd co-doped ZnO was studied in UV-vis region using Diffuse Reflectance Spectroscopy (DRS) between 200 and 800 nm.

2.3.4. Photocatalysis

ZnO powders (1 g/L) and La-Nd co-doped ZnO nanospheres (1 g/L) were dispersed in RR24 and RY145 solutions of concentration 10 mg/L separately and placed in photochemical reaction apparatus, then magnetically stirred under dark conditions and the absorbance of the solution was measured every 15 min until the dark adsorption equilibrium was achieved. Later, the 120W mercury lamp was used as the light source, the solutions were UV irradiated with constant stirring, samples in different reaction times were collected and centrifuged for 10 min at 6000 rpm, the absorbances of obtained supernatants were examined by using Shimadzu-UV3600 spectrophotometer. Furthermore, the actual percentages of degradation could be calculated after the adsorptions were eliminated according to formula (1):

$$R = \frac{A_0 - A}{A_0} \times 100\% \quad (1)$$

where, A is the instant absorbance and A_0 is the initial absorbance.

2.2.5. Effluent treatment containing reactive dyes

Discard solutions of RR24 and RY145 were simulated according to the following formula, the structural of RR24 and RY145 as shown in Fig. 1. RR24 liquor: RR24 10 mg/L, sodium chloride 0.4 g/L, sodium carbonate 0.3 g/L, peregal O 8 mg/L, penerating agent JFC 20 mg/L and deionized water; RY145 liquor: RY145 10 mg/L, sodium sulphate 0.3 g/L, sodium carbonate 0.2 g/L, peregal O 8 mg/L, penerating agent JFC 20 mg/L and deionized water. All the materials were heated at 65℃ to obtain a simulated discard solutions and adjust the system PH to 8.

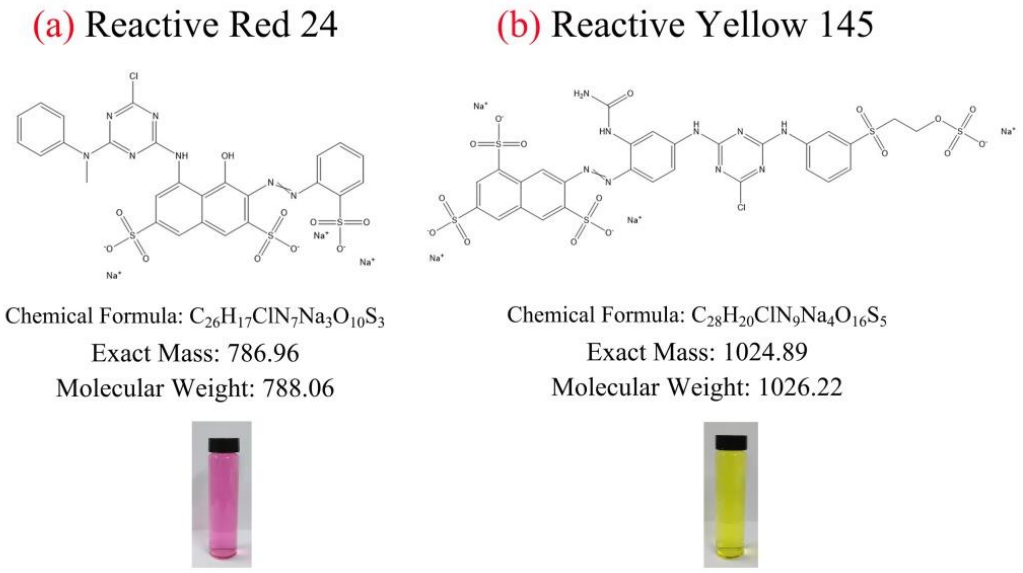

Fig. 1. Structural formulae of (a) reactive red 24 and (b) reactive yellow 145.

3. Results and discussion

3.1. Scanning electron microscopy (SEM)

The surface morphologies of the different morphologies ZnO was examined by SEM, as shown in Fig. 2. ZnO nanosheets with 300~400 nm of lengths and 10±1 nm of thicknesses in Fig. 2a were obtained without ethylene glycol as morphology controller.

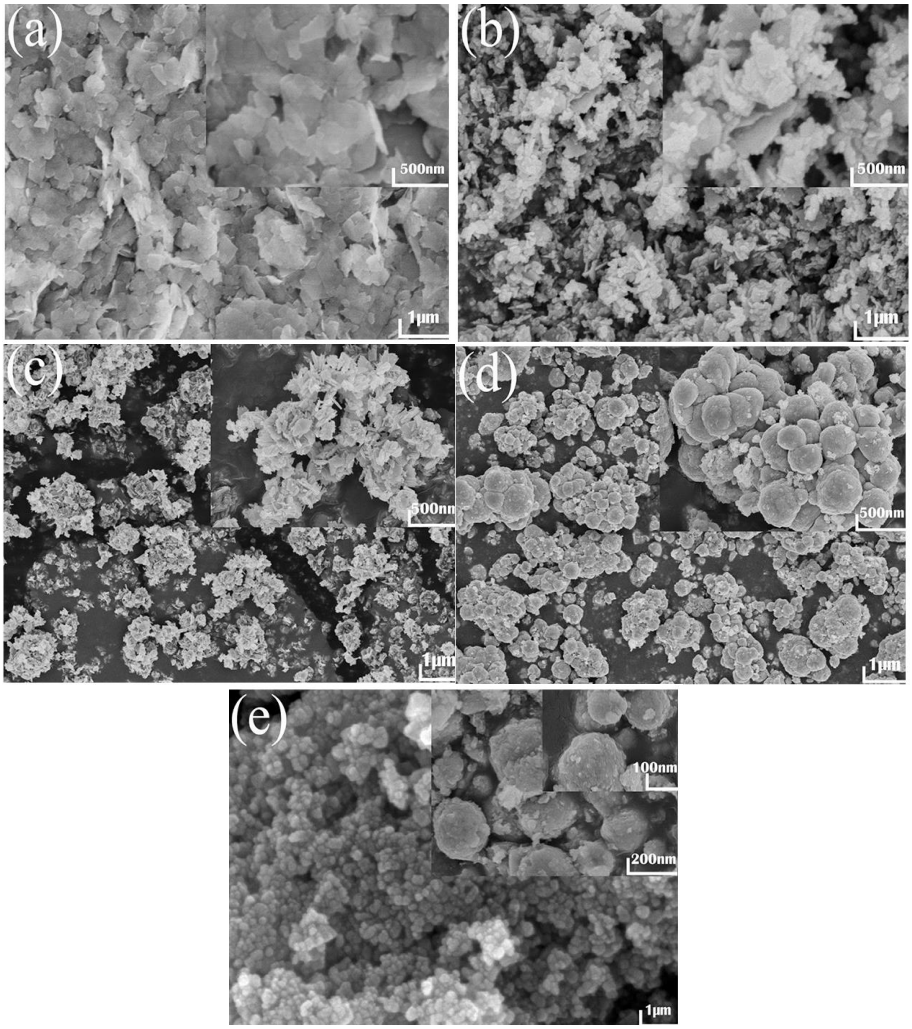

Fig. 2. SEM images of different morphologies ZnO: (a) minor size flake without EG, (b) superior size flake with n_{EG}/n_{Zn} at 50:1, (c) globose flower with n_{EG}/n_{Zn} at 100:1, (d) cauliflower with n_{EG}/n_{Zn} at 150:1 (e) sphere with n_{EG}/n_{Zn} at 200:1.

As the scale of EG/Zn increased to 50:1, lamellar structures grown more completely, meanwhile lengths of nanoflakes reduced to 200~300 nm (Fig. 2b). The morphology in Fig.2c was generated when the ratio of n_{EG}/n_{Zn} (molar ratio of ethylene glycol to zinc chloride) was 100:1, three-dimensional spherical flowers with 1500~2000nm of diameters ulteriorly formed from two-dimensional flakes due to the enhancement of ambient pressure. As shown in Fig. 2d, the morphology of cauliflower was observer which has similar length and width of particle as spherical nanoflowers, gained at 150:1 of n_{EG}/n_{Zn}. Then, as n_{EG}/n_{Zn} reach 200:1, the pressure of system enhanced further, what followed was the appearance of nanospheres with 90~130 nm of diameters (Fig. 2e), relatively considerable specific surface area is possessed by this sample due to its morphology, size and extremely rough surfaces of the spheres, which endowed the material with remarkable photocatalysis. Therefore, compared with other samples, spherical ZnO has preferable photocatalytic activity in theory.

3.2. X-ray diffraction (XRD)

The ZnO was structurally characterized by XRD in Fig.3, which shows X-ray diffraction patterns of single ZnO and La-Nd co-doped ZnO in different ratio. Sharp-pointed diffraction peaks appear at (100), (002) and (101) planes unexceptionally in XRD patterns of ZnO samples displayed in Fig. 3a, which shows good agreement with the hexagonal wurtzite zinc oxide (JCPDS file no. 36-1451) [26]. The size of ZnO nanosphere was calculated by the Debye-Scherrer formula

about 97.58nm. In addition, none of impurity peaks were observed in the spectrum, indicating that the prepared ZnO particles were relatively pure.

XRD of La-Nd co-doped zinc oxide was shown in Fig. 3b, demonstrates that all the samples were provided with hexagonal crystal structure. In contrast, pattern of 2%La-1%Nd/ZnO has sharper characteristic peaks with superior Full Width at Half Maximum (FWHM) at 31.79 º, 34.48 º and 36.51 º respectively [27], indicates minor grain size and higher crystallinity. Refer to significant intensities and shifts of peaks, most of La^{3+} and Nd^{3+} incorporated into the crystal lattice of ZnO, possessed the position of Zn^{2+}, the rest located in the interstitial space of lattice or attached to crystal surface. For samples with other doping ratios, diffraction peaks shift to lower angles while growing indistinctively [28], confirm the formation of recombination centres owing to the reduction of carriers' capture bit spacings [29], which has inhibited the separation of photogenerated electrons and holes, further reduced the photocatalytic activity. Therefore, the optimal incorporating ratio of La-Nd to zinc oxide for photocatalysis was considered to be 2%-1%.

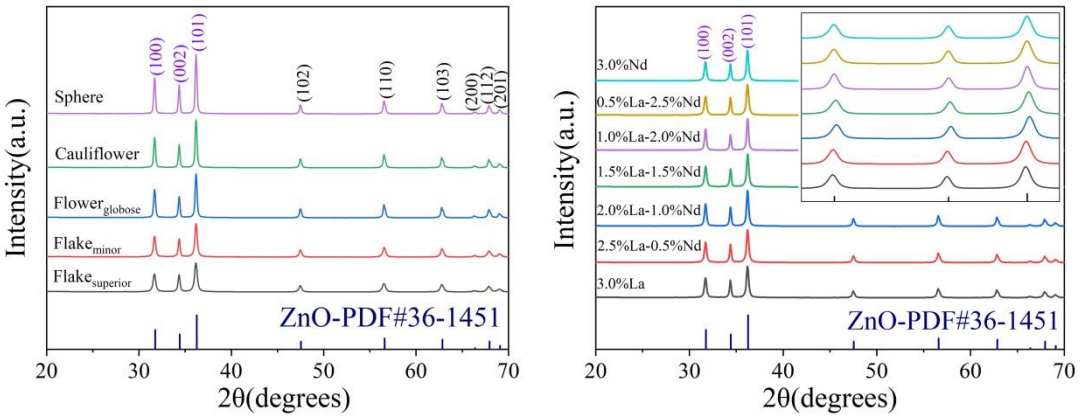

Fig. 3. The XRD patterns of single ZnO (a) and La-Nd co-doped ZnO (b).

3.3. X-ray photoelectron spectroscopy (XPS)

In order to research the elemental composition and chemical state of 2% La-1% Nd co-doped ZnO surface, XPS was performed on the materials. The results were shown in Fig. 4, all XPS spectra were calibrated using C 1s. As shown in Fig. 4b, the high peaks located at 1021.54 eV and 1044.66 eV were corresponding to Zn $2p_{3/2}$ and Zn $2p_{1/2}$, the difference of binding energy between the peaks was 23.12 eV, which was accorded with the standard value of ZnO [30]. Fig.4c was the high-resolution scan XPS of La 3d, the La 3d core level spectra for the 2% La-1% Nd co-doped ZnO sample split into La $3d_{3/2}$ and La $3d_{5/2}$ due to a spin-orbit interaction, and each line was splits into a main line and a “shake-up” satellite line, the difference of energy between the main line and “shake-up” satellite line was 3.72 eV, proved that La mainly exists in the form of La^{3+} in the composites [31]. As for high-resolution Nd 3d spectrum, as shown in Fig. 4d, the peaks at 982.21 eV and 1002.35 eV assigned to Nd $3d_{5/2}$ and Nd 3d $_{3/2}$, the peaks at 977.78 eV, 995.93 eV and 1008.69 eV were the satellite peaks of Nd 3d for doped ZnO [32]. XPS results confirmed the successful doping of La and Nd.

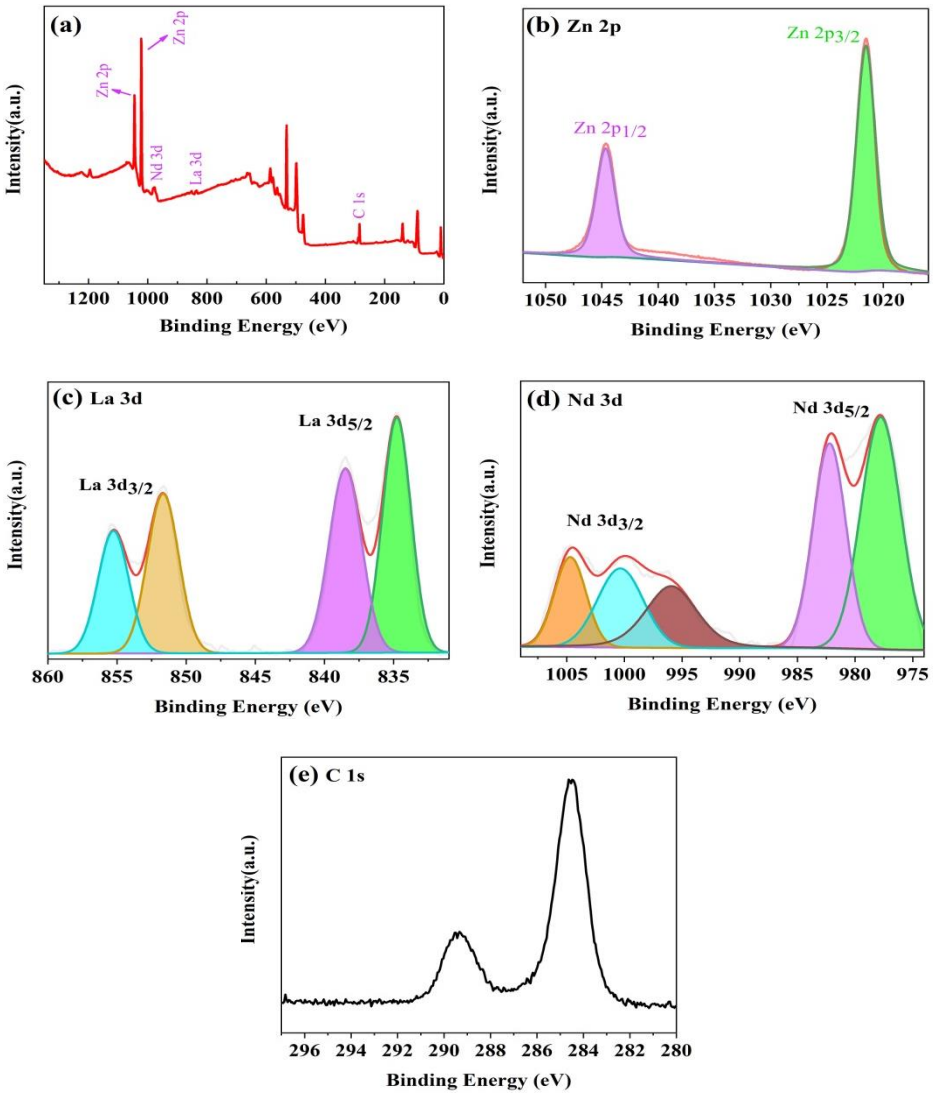

Fig. 4. XPS spectra of 2%La-1%Nd co-doped ZnO nanosphere: (a) survey scan, (b-e) high resolution scans Zn 2p, La 3d, Nd 3d and C 1s respectively.

3.4. Diffuse reflection spectrum (DRS)

In order to research the change of La and Nd co-doping on ZnO band gap, DRS was performed on ZnO and 2%La-1%Nd co-doped ZnO. Fig. 5a shows the absorption spectra of ZnO and 2%La-1%Nd co-doped ZnO were obtained from UV-vis diffuse reflectance data by calculation of the Kubelka-Munk equation. Compared to ZnO, the 2%La-1%Nd co-doped ZnO revealed obviously enhance light absorption in the region of 400-800 nm and shown enormous absorption intensity, this phenomenon was due to the formation of impurity levels in the ZnO band gap caused by La and Nd doping. The band gap of ZnO and 2%La-1%Nd co-doped ZnO was calculated by Tauc's formula, as shown in Fig. 5b. For the undoped ZnO, the band gap was calculated as 3.23 eV, by contract, the value was decreased to 2.98 eV for 2%La and 1%Nd co-doped. DRS results demonstrate the effectively reduced of ZnO band gap and was expected to improve the photocatalytic activity.

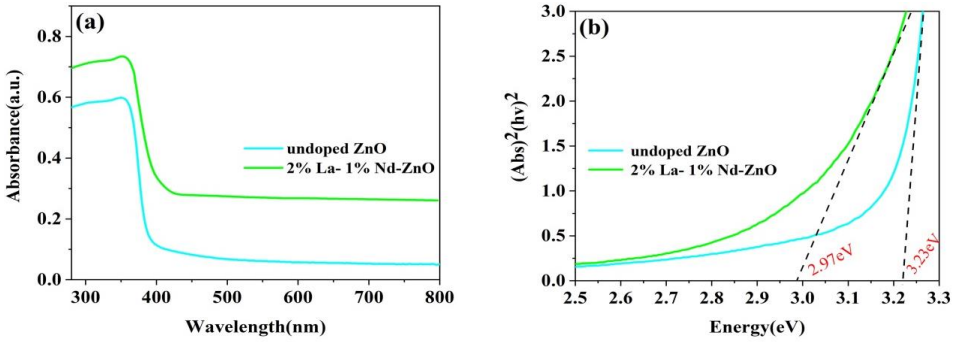

Fig. 5. UV-vis absorbance spectra of undoped ZnO , 2%La-1%Nd co-doped ZnO (a) and Tauc plots (b).

3.5. Dark adsorption

Fig. 6 showed the result of dark adsorption, the equilibrium achieved after 30 min of adsorption to RR24 for all the samples in Fig. 6a. In comparison, spherical ZnO shows better effect of sorption, manifests as 1.7% of the adsorption rate, due to comparatively appreciable specific surface area, while using the material to degrade RY145, 45 min would be required for reaching the balance and 5.1 of adsorption percentage, as shown in Fig. 6b. The diversities were attributed to more active groups of RY145 solution than in liquor of RR24, which provide active centres for the participation of sorption, further cause significant increase of adsorption and prolongation of the process to achieve equilibrium.

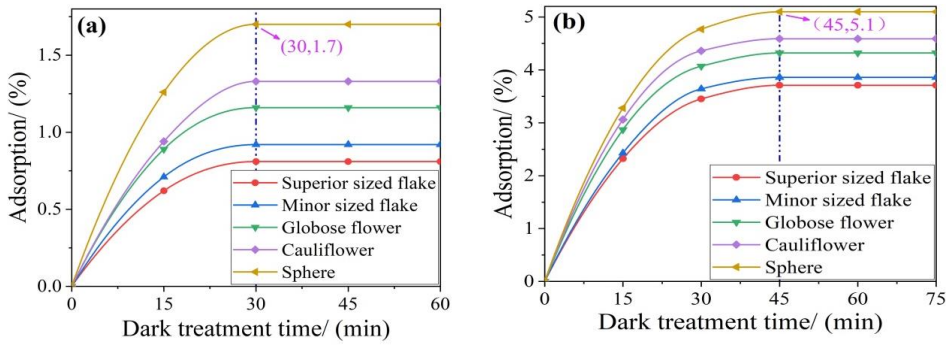

Fig. 6. Adsorptions of (a) RR24 and (b) RY145 by ZnO.

3.6. Photocatalysis

The dyes degradations in pure solutions and effluent liquors of samples were shown in Fig. 7. Degradations of both dyes in control group were less than 0.1 percent after 120 min of irradiation, indicated that ultraviolet itself has little or no connection with the decomposition of dyes. While looking into Fig. 7a, all degradations of RR24 increase with time constantly in the whole process, and this trend exhibits significantly in the first 30 minutes. Among the samples, nanospheres shown relatively substantial photocatalytic activity, almost degraded RR24 completely under ultraviolet irradiation for 120 min, and made the degradation of RY145 reach 96.21% in the same period of time (Fig. 7b). In addition, the slightly lower parameter of RY145 was attributed to its more complicated molecular structure. Consequently, spherical ZnO represents comparatively considerable activity of photocatalysis while possessing larger specific surface area, and the conclusion is accordant with the inference in morphology analysis.

As it can be seen in Fig. 7c, after being doped with the La, significant improvement of photocatalysis endowed to the materials, owing to the difference of Fermi energies [33] between ZnO and the metal ions, which leads to the electron movement, effectively reduces the consumption caused by recombination of electron-hole pairs and prolongs the existence time of carriers [34-35]. In contrast, 2%La-1%Nd co-doped ZnO shown appreciable performance of

degradation to RR24, almost degraded the dye completely after 60 min of UV irradiation. Meanwhile, the material also performed preferably to RY145, reached 99.99% of degradation rate when the other conditions remained invariant (Fig. 7d), it can be proved form this result that the doping of La and Nd effectively reduced the band gap of ZnO and decreased the energy required for electron transition, which was consistent with the DRS results. Through observation, the photocatalysis of ZnO was affected by the incorporating amounts of La and Nd, showing visible regularity. While analysing single element, the photocatalytic activity of composite only increases with the rise of doping ratio in a certain range, however, when the critical value was exceeded, a decline of catalytic capacity occurs, which was caused by ions due to the limitation of solubility in incorporation, then the majority of electrons and holes concentrate on the surface of ZnO owing to the sedimentation of excessive ions, meanwhile the photocatalysis was abated through the recombination of carriers. In conclusion, the optimal doping ratio of La-Nd for spherical ZnO was determined to be 2%-1%, which was consistent with the theoretical result obtained in the analysis of crystal structure, compound with such ratio was provided with excellent photocatalytic activity, shows substantial degradation effect of reactive dyes.

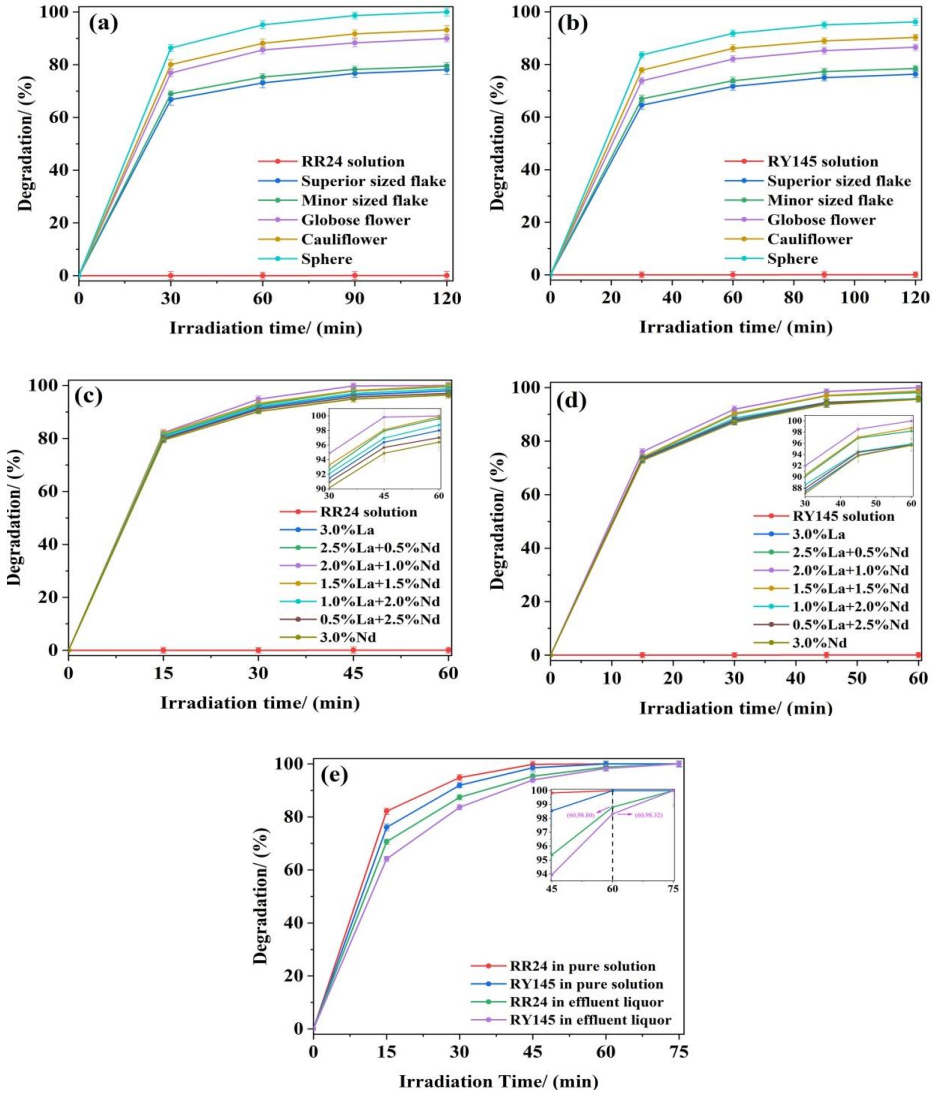

Fig. 7. Dye degradations in pure solutions and effluent liquors: (a) single ZnO in pure solutions, (b) single ZnO in effluent liquors, (c) La-Nd co-doped in pure solutions, (d) La-Nd co-doped in effluent liquors and (e) difference degradations of RR24 and RY145 in pure solutions or effluent liquors.

Compared with degradations of RR24 and RY145 in pure solutions, inferior effects were observed in Fig. 7e of the same dyes in discard liquids, due to the addition of several inorganic sodium salts, which imported abundant Na^+ into the liquors, and inhibited the degradation of dyes by promoting the aggregation of molecules [36].Although it was confirmed that the presence of sodium salts acts as an interfering factor, the effect was relatively acceptable, as the expected degradation could be achieved by prolonging the process of photocatalysis. For instance, RR24 was almost totally degraded in pure solution after 60 min of UV irradiation, while only attaining 98.80 percent in 205 effluent liquors, nevertheless, the rate of degradation still reached 99.99% when the time of reaction was extended to 75 minutes. In addition, similar conclusion could be obtained through analysing the same situation of RY145, thus it was demonstrated that 2%La-1%Nd co-doped ZnO continues to possess exceptional photocatalytic activity with the interference of sodium salts.

3.7. Removal of organic pollutants

Without exception, COD_{Cr} (potassium dichromate method) curves of two effluent liquors in Fig. 8a contain significant peaks at 15 min and maintain downward trends in subsequent irradiation time, as high COD was mainly caused by dyes and surfactants [40]. Among these components, penetrating agent JFC and peregal O were found to be fatty alcohol polyoxyethylene ethers with different degrees of polymerization, could be oxidized without difficulty, however, macromolecules of RR24 and RY145 were hard to be completely decomposed. In the first 15 minutes, molecular structures of dyes were destroyed with the oxidation of hydroxyl radicals, meanwhile, generated micromolecular substances which could be oxidized by potassium dichromate led to remarkable increases of COD. During the subsequent process, micromolecular organics were further mineralized by radicals, then continuous decreases of COD observed [41]. Eventually, 76.68% and 76.32% of removal efficiencies were achieved for discard solutions of RR24 and RY145 separately after 120 min of ultraviolet treatment, therefore, it was testified that 2%La-1%Nd co-doped ZnO possesses appreciable ability of orgnic elimination.

As it shown in Fig. 8b, constant downsides occur in both TOC curves along with the extension of degradation time, owing to the conversion from macromolecules to minor orgnics, which was promoted by the strand breaking of polyoxyethylene ethers and the destruction of dye molecules, and then generated substances were ulteriorly oxidized to mineralizations [42]. Under UV irradiation for 120 min, removal efficiencies of TOC have respectively attained 73.16% and 72.36% for effluent liquors containing RR24 and RY145. Consequently, 2%La-1%Nd co-doped ZnO was provided with significant photocatalytic capacity of organic removal in discharge liquids of reactive dyes, and the conclusion was accordant with the inference obtained through COD analysis.

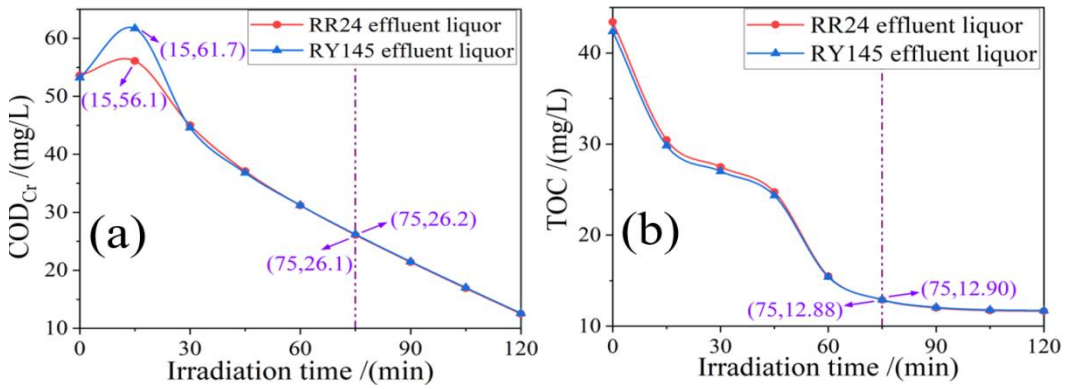

Fig. 8. (a) CODcr and (b) TOC of effluent liquors containing reactive dyes.

4. Conclusions

Nanospheres and other morphologies of ZnO were prepared with solvothermal method by controlling the molar ratio of ethylene glycol and zinc at 200:1, among these samples, spherical ZnO reached 96.21 and 99.99 of degradation percentages separately to RY145 and RR24 under ultraviolet irradiation for 120 min, which proved that the material had significant photocatalytic activith. New compounds were obtained by incorporating different proportions of La-Nd to the produced nanospheres, meanwhile the optimum doped ratio of La-Nd was determined to be 2%-1%. Compared with undoped ZnO, the band gap of 2%La-1%Nd co-doped ZnO decreased from 3.23 eV to 2.97 eV and sample shown remarkable improvements of photocatalysis with little variety of lattice. Through 60 min of UV illumination, the degradations of both RR24 and RY145 were accomplished when 2%La-1%Nd co-doped ZnO was served as catalyzer, demonstrated the splendid photocatalytic ability of the material.

While using 2%La-1%Nd co-doped ZnO in UV treatment of RR24 and RY145 effluent liquors, dye was almost completely degraded in each liquid at 75 min. After photoreaction for 120 min, 76.68% and 73.16% of chemical oxygen demand and total organic carbon removal efficiencies were achieved respectively for RR24 discard solution, as for discharge liquor of RY145, 76.32 and 72.36 removal percentages of COD and TOC were separately attained at the same time. Thus, it was confirmed that ZnO nanospheres doped with 2%La-1%Nd possess appreciable removal capacity of orgnic 259 pollutants in the degradation of effluent liquors containing reactive dyes.

Acknowledgments

Appreciate for the laboratory and equipments provided by Shanghai University of Engineering Science and XPS, XRD analysis were provided by Shiyanjia Lab (www.shiyanjia.com). Meanwhile, thanks to Dr. Wang Liming, Dr. Xu Lihui, Dr. Shen Yong, Mr. Xie Mingrui and Ms. Hao Huimin for their help and suggestions.

The research was funded by National Natural Science Foundation of China (project 51703123), Shanghai Natural Science Foundation(21ZR1426200) and Graduate Research innovation Fund of Shanghai University of Engineering Science(20KY0906).

References

[1] B. Krishnakumar, F. A. Alsalme, Alharthi, D. Mani et al., Optical Materials 113 (2021).
[2] P. Basnet, D. Samanta, T. Chanu et al., Journal of Alloys and Compounds, 867 (2021).
[3] S. Kalaiarasan, P. Uthirakumar, D. Shim et al., Environmental Nanotechnology, Monitoring & Management, 2021.
[4] Y. Mishra, R. Adelung, Materials Today, 2017.
[5] R. Saravanan, H. Shankar, T. Prakash et al., Materials Chemistry and Physics **125**(1), 277 (2010).
[6] F.-C. Liu, J. Yong Li, T. H. Chen et al., Materials **10**(7), 2017.
[7] A. Nicolay, A. Lanzutti, M. Poelman et al., Applied Surface Science **327**, 379 (2015).
[8] Nastaran Kalanpour, Saeid Nejati, Sajjad Keshipour, Journal of the Iranian Chemical Society **5**(18), 1243 (2020).
[9] Sajjad Keshipour, Kamran Adak, Iranian Journal of Chemistry and Chemical Engineering **3**(37), 23 (2018).
[10] K. M. Lee, C. W. Lai, K. S. Ngai et al., Water Research **88**, 428 (2016).
[11] Wang Kaixiang, Wei Tingting, Li Yinuo, He Li, Lv Yin, Chen Long, Ahmad Ayyaz, Xu Yisheng, Shi Yulin, Chemical Engineering Journal, 413 (2012).
[12] R. Nithya, S. Ragupathy, D. Sakthi et al., Chemical Physics Letters, 755 (2020).

[13] B. U. Hosaholalu, A. Sannaiah, M. B. Nandaprakash, Chemical Data Collections, 24 (2019).
[14] E. Christy, S. Jackcina, A. Amalraj et al., Environmental Chemistry and Ecotoxicology **3**, 31 (2021).
[15] U. Alam, A. Khan, D. Ali et al., Rsc Advances **8**(31), 17582 (2018).
[16] J. E. Morales-Mendoza, F. Paraguay-Delgado, Materials Letters, 291 (2021).
[17] Li Bo Yan, Liu Fang Fang, Lin Lie, Optoelectronics Letters **16**(6), 451 (2020).
[18] Narkhede Nilesh, Zheng Huayan, Zhang Huacheng, Zhang Guoqiang, Li Zhong, ChemCatChem **12**(22), 5697 (2020).
[19] S. Baruah, J. Dutta, Adv. Mater. **10**(01301), 789 (2009).
[20] M. Giahi, S. Habibi, S. Toutounchi, et al., Russian Journal of Physical Chemistry A **86**(4), 689 (2012).
[21] A. Rosset, K. Djessas, V. Goetz et al., RSC Advances **10**, 25456 (2020).
[22] A. Serrà, Y. Zhang, B. Sepúlveda et al., Water Res. **169**, 115210 (2020).
[23] R. Amiruddin, K. Santhosh, Ceramics International **40**(7), 11283 (2014).
[24] W. Vallejo, A. Cantillo, B. Salazar et al., Catalysts **10**, 5(2020).
[25] G. Vilardi, L. D. Palma, N. A. Verdone, Chemosphere **220**, 590 (2019).
[26] P. P. Mahamuni, P. M. Patil, M. J. Dhanavade et al., Biochem. Biophys. **17**, 71 (2019).
[27] P. Singh, R. Kumar, R. K. Singh, Ind. Eng. Chem. Res. **58**, 17130 (2019).
[28] A. Javaid, M. B. Tahir, M. Sagir et al., Ceramics International **46**(8), 11955 (2020).
[29] R. M. Jagtap, D. R. Kshirsagar, V. H. Khire et al., Journal of Solid State Chemistry **276**, 194 (2019).
[30] D. S. Vasanthi, K. Ravichandran, P. Kavitha, S. Sriram, P. K. Praseetha, Superlattices and Microstructures 145 (2020).
[31] Zhang Yiqun, Wang Chong, Zhao Lianjing, Liu Fengmin, Sun Xiaoying, Hu Xiaolong, Lu Geyu, Sensors and Actuators: B. Chemical, 334 (2021).
[32] T. Indumathi, C. Theivarasu, I. Pradeep, Rani M. Thillai, G. Magesh, Rahale C. Sharmila, Kumar E. Ranjith, Surfaces and Interfaces 23 (2021).
[33] C. Wei, J. P. Xu, S, Shi et al., Journal of Colloid And Interface Science **577**, 279 (2020).
[34] U. H. Balakrishna, A. Sannaiah, Chemical Data Collections, 2021.
[35] Y. Liu, Q. Zhang, H. Yuan et al., Journal of Alloys and Compounds, 868 (2021).
[36] Jin Xin, Wang Rui, Jin Peng Kang, Shi Xuan, Wang Yong, Xu Lu, Wang Xiaochang, Xu Huining, Chemical Engineering Journal, 413 (2021).
[38] H. J. Ali, S. A. Ahmed, Colloids and Surfaces A: Physicochemical and Engineering Aspects, 605 (2020).
[39] Baş, T. Ergan, G. Erhan, Journal of Environmental Chemical Engineering **8**(5), 2020.
[40] U. A. Toor, T. T. Duong, S. Y. Ko et al., Journal of Environmental Management, 2020.